Forest Fire Detection: Cross-Sensor Transfer Learning with DenseNet-121 from Landsat-8 to Sentinel-2 Satellite Imagery in Benguet, Philippines

Lance Asher M. Elloso, Estefanee Ashley N. Garcia, Khristine F. Mecija, and John Paul Q. Tomas*

School of Information Technology, Mapúa University, Makati City, Philippines
Email: lamelloso@mymail.mapua.edu.ph (L.A.E.); eangarcia@mymail.mapua.edu.ph (E.A.G.);
kfmecija@mymail.mapua.edu.ph (K.F.M.)
*Correspondence: jpqtomas@mapua.edu.ph (J.P.T)

***Abstract*—Timely Forest fire detection is critical for mitigating ecological and economic losses, yet developing nations often lack the extensive labeled datasets required for deep learning models. This study investigates a cost-effective, cross-sensor transfer learning framework using DenseNet-121 to detect forest fires in Benguet, Philippines. By pre-training on a large-scale global Landsat-8 dataset and fine-tuning on a limited, locally curated Sentinel-2 dataset, the model overcomes data scarcity and sensor-specific limitations. The proposed method achieved an F1-score of 89.47% on unseen Sentinel-2 imagery, outperforming direct transfer learning baselines by reducing false positives by over 28%. Furthermore, the integration of Gradient-weighted Class Activation Mapping (Grad-CAM) provides interpretable heatmaps for spatial severity estimation, bridging the gap between binary classification and operational situational awareness. These results demonstrate a scalable, transparent, and highly accurate solution for environmental monitoring in data-constrained regions.**

***Keywords*—Forest Fire Detection, Cross-Sensor Transfer Learning, DenseNet-121, Convolutional Neural Network, Remote Sensing, Landsat-8, Sentinel-2, Satellite Imagery.**

I. Introduction

Forest fires are uncontrolled combustions of natural vegetation that can rapidly destroy woodland areas. They have increased in extent and severity in recent years, driving substantial ecological and socio-economic impacts worldwide, which underscores the need for timely detection and response [1, 2]. In recent years, the increasing frequency of forest fires has been largely attributed to anthropogenic activities, intensive land use, rising global temperatures, and climate change. Wildfires often go undetected until they have grown large enough to be identified, and in certain instances, they may be challenging to detect or remain entirely unnoticed. These fires pose significant threats not only to ecosystems but also to human livelihoods, making the development of effective detection and monitoring systems an urgent priority.

Satellite remote sensing offers routine, large-area monitoring with multispectral observations, well suited for active fire detection and situational awareness. Sensors such as Landsat-8 and Sentinel-2 enable extraction of spectral cues associated with high-temperature combustion and fire effects at frequent revisit intervals. [3]. Globally, researchers have emphasized the importance of innovations in early wildfire detection to mitigate environmental and economic losses. For instance, Ghali and Akhloufi [4] underscored the value of deep learning systems for wildfire detection and prediction, comparing various deep learning methods for wildfire detection and prediction using satellite data, noting that Convolutional Neural Networks (CNNs) are effective at detecting and classifying fires in satellite imagery. Similarly, Pereira *et al.* [3] emphasized that while deep learning approaches using satellite imagery such as Landsat-8 show promise, the scarcity of labeled datasets limits model stability and transferability. This presents a critical research opportunity, the design of models capable of leveraging cross-sensor transfer learning to maximize the use of existing data.

Several studies have successfully applied deep learning models for forest fire detection using satellite data, achieving promising results [5-15]. For instance, Rostami *et al.* [16] used Landsat-8 data and deep multiple kernel learning, achieving a fire detection precision of 95.71%, such findings highlight the potential of machine learning methods for accurate forest fire detection. However, the effectiveness of deep learning models is highly dependent on large, well-annotated datasets, which are often scarce for certain geographic areas or sensor types. This limitation is particularly challenging for developing countries like the Philippines, where resources for dataset development are limited.

Despite experiencing significant tree cover loss due to forest fire, the Philippines still lacks a centralized forest fire detection system. Reports from the Asian Forest Cooperation Organization (AFoCO) in 2021 highlighted challenges such as limited technological capacity, bureaucratic inefficiencies, and prevalent anthropogenic causes like slash-and-burn farming [17]. In the absence of a centralized forest fire detection system, the country primarily relies on weather monitoring services from the Philippine Atmospheric, Geophysical and Astronomical Services Administration (PAGASA) for weather and temperature data signaling the arrival of the summer season, rather than a dedicated fire monitoring technology. This significantly limits the ability to detect and respond to forest fires promptly, increasing the risk of ecological damage and unreported fire incidents. This growing management challenge calls for stable detection and monitoring capabilities. Regional initiatives have emphasized integrating early warning, near real-time detection, and reporting into operational forest fire management, reflecting capacity needs and the value of interoperable information systems for rapid, coordinated responses.

To address these gaps, this study investigates the application of DenseNet-121, a convolutional neural network (CNN), as the core classifier for forest fire detection in Benguet, Philippines. DenseNet-121 is selected for its strong feature propagation, feature reuse, and parameter efficiency, which support transfer learning, high-accuracy recognition tasks [18] and its effectiveness on other studies [12, 19-21]. The study explores cross-sensor transfer learning by adapting features learned from Landsat-8 to Sentinel-2 imagery. Sentinel-2 provides comparable multispectral bands and spatial resolutions (10–60 meters) with a shorter revisit time of 5 days, offering a suitable and timely platform for local fire detection efforts. The research specifically targets Benguet province to assess the feasibility and reliability of using DenseNet-121 for accurate fire detection under limited local training data conditions.

By integrating cross-sensor transfer learning with Sentinel-2 imagery, this study aims to develop a stable, generalizable, and cost-effective forest fire detection system for the Philippines. This pioneering approach holds the potential to establish a precise and dependable methodology that can mitigate unreported incidents and facilitate timely emergency response. Furthermore, this work serves as a valuable framework for future remote sensing and environmental monitoring research, particularly in data-scarce regions.

This study addresses the critical gap in applying deep learning to data-scarce regions by validating a cross-sensor transfer learning protocol. The specific contributions of this work are:

1. **Cross-Sensor Domain Adaptation:** Demonstrating that features learned from global Landsat-8 data can be effectively transferred to Sentinel-2 imagery to solve local data scarcity issues.
2. **Operational Reliability:** Achieving a significant reduction in false positive rates compared to standard training methods, crucial for resource-limited fire response.
3. **Explainable Severity Assessment:** Introducing a Grad-CAM-based framework that converts "black box" model predictions into interpretable, area-based severity estimates for decision support.

II. Literature Review

A. Forest Fire Detection Using Satellite Imagery

Early research of Alkhatib [22] in forest fire detection relied heavily on traditional remote sensing techniques, employing threshold-based algorithms on thermal and multispectral data. While these approaches provided foundational insights, they often detected fires only after they had become widespread and uncontrollable, leading to devastating environmental and economic losses. It emphasized the limitations of these early systems, which primarily utilized optical sensors, digital cameras, and wireless sensor networks alongside satellites, stressing the urgent need for more effective early detection methods.

To address these shortcomings, Pereira *et al.* [3] developed a large-scale dataset for active fire detection using Landsat-8 imagery, comprising over 150,000 image patches processed with established handcrafted algorithms from Schroeder *et al.* [23], Murphy *et al.* [24], and Kumar and Roy [25]. This dataset enabled the application of deep learning models on a global scale, significantly advancing the accuracy and scalability of fire detection. Building on this foundation, Rostami *et al.* [16] introduced a deep multiple kernel learning model, MultiScale-Net, which leveraged spectral-spatial features from SWIR and blue bands. Their approach achieved a precision of 95.71%, demonstrating the potential of CNN-based architecture for detecting active fires across diverse regions.

Further innovation was presented by Zhonghua *et al.* [10] who proposed FireCNN using Himawari-8 satellite data. Their model integrated multi-scale convolution and residual learning, improving detection accuracy by 35.2% compared to traditional thresholding methods, even when trained on a relatively small dataset. Similarly, Nabi and Bordanov [26] highlighted the inefficiency of segmenting entire fire regions due to their rapidly changing shapes and sizes. Instead, they argued that confirming the presence of a fire source is more critical for operational decision-making. Their study, which evaluated multiple ANN architectures on Landsat-8 and Uruguay datasets, achieved 99% classification accuracy by prioritizing minimal input channels, demonstrating CNNs' adaptability in resource-constrained environments.

B. Deep Learning for Fire Detection

Deep learning has emerged as a transformative approach for remote sensing-based fire detection, particularly using CNN. Huang *et al.* [18] introduced DenseNet, a deeply supervised architecture designed to mitigate vanishing gradients and improve feature propagation via dense connectivity. Trained on the ImageNet dataset [27], DenseNet demonstrated superior performance over deeper

ResNet models while requiring fewer computational resources. Specifically, DenseNet-121 achieved a consistent 98% accuracy rate across multiple remote sensing benchmarks including EuroSAT, UC Merced-Land Use and NWPU-RESISC45 datasets [19], validating its suitability for high-dimensional satellite imagery analysis, where efficiency and accuracy are paramount.

Priya and Vani [28] utilized Inception-v3 combined with transfer learning to classify fire and non-fire satellite images, further enhancing detection through local binary pattern analysis. Their approach reduced false positives and achieved high precision and recall scores, illustrating the effectiveness of combining deep architectures with feature-based refinements. Additionally, Minetto *et al.* [21] and Li *et al.* [12] validated DenseNet's robustness by applying it to large-scale benchmark datasets such as FMOW [29] and NWPU-RESISC45 [20, 30], confirming its strength as a universal feature extractor across multiple remote sensing domains.

Recent advancements in computer vision have increasingly focused on unified architectures that combine classification with detailed spatial understanding. For instance, the Panoptic-Aware Object-Wise Depth Estimation (PODE) model [31] demonstrates the efficacy of joint feature learning, utilizing Feature Pyramid Networks to simultaneously perform panoptic segmentation and depth estimation for occlusion prediction. While applied to depth estimation, this principle of leveraging unified deep networks to extract multi-dimensional spatial context aligns with the objectives of modern remote sensing. Similarly, our study adopts this trend by integrating DenseNet-121 not just for binary fire classification, but effectively as a backbone for spatial severity estimation via Grad-CAM, thereby deriving rich, actionable insights from single model architecture.

C. Transfer Learning in Remote Sensing

While deep learning models require large amounts of labeled data, the scarcity of annotated satellite imagery poses a significant challenge. Iman *et al.* [30] discussed how Deep Transfer Learning (DTL) addresses this limitation by reusing pre-trained models, reducing training costs, and improving performance in low-data scenarios. This strategy is particularly advantageous in forest fire detection, where compiling diverse and labeled datasets can be costly and time-consuming. Priya and Vani [28] demonstrated this advantage by employing transfer learning with Inception-v3 to achieve improved fire classification accuracy using limited datasets.

D. Cross-Sensor Adaptation and Limitations

Cross-sensor adaptability remains a critical area of research, given the variability in spectral and spatial characteristics across satellite platforms. Lopez-Puigdollers *et al.* [32] explored this challenge in cloud detection, evaluating models trained on Landsat-8 and testing them on Sentinel-2. Their findings confirmed the feasibility of cross-sensor transfer when using fully convolutional architectures, provided that dataset diversity and spatial variability are adequately addressed. Extending these principles, Zhao *et al.* [6] proposed a model for detecting fire smoke across multispectral datasets from Landsat and Sentinel-2. Furthermore, a model by Zhao *et al.* [33] demonstrated that incorporating an Input Amplification (IA) module which adapts class-specific spectral patterns learned from one sensor could effectively resolve bands discrepancies. This framework achieved significantly higher cross-domain performance than models trained exclusively on target Sentinel-2 data, demonstrating that the IA module effectively retains and transfers critical spectral features from the source dataset. This approach is model-agnostic and offers a scalable solution for multi-sensor fire detection.

E. Local Research Context

While global deep learning research demonstrates high accuracy in fire detection using satellite imagery, the local context in the Philippines shows a reliance on traditional methods and susceptibility modeling.

A study by Poclis *et al.* [34] compared fire susceptibility models in Benguet province. A region highly prone to fires, found that indices such as the Hybrid Fire Index (HFI) and Fire Risk Index (FRI) were effective in identifying high-risk areas. However, this study noted that continued need for research into the long-term ecological and socio-economic impacts of these fires.

Similarly, local applications utilizing Earth Observation data have focused on damage assessment. Canlas *et al.* [35] utilized remote sensing data, including *Sentinel-2 imagery* and data from the Diwata-2 micro-satellite, to estimate burned forest areas in Benguet using traditional methods like Support Vector Machine (SVM) classification and Normalized Difference vegetation Index (NDVI) thresholding. This research highlighted the value of small-scale space missions for cost-effective disaster assessment in developing nations.

In Tarlac, Baloloy *et al.* [36] focused on detecting and quantifying burn severity in sugarcane plots using Landsat imagery and the Differenced Normalized Burn Ratio (dNBR), achieving an 89.03% accuracy rate in classifying burned and unburned areas. Separately, efforts by Lerios *et al.* [37] to predict fire incidents in urban settings like Laguna province employed Recurrent Neural Networks (RNN) using historical Bureau of Fire Protection (BFP) incident data, demonstrating the potential of machine learning for pattern recognition in disaster management.

Collectively, these studies confirm the fire risk severity in regions like Benguet and Tarlac. It demonstrates the foundational use of satellite data and non-deep-learning classifiers (SVM, indices, RNNs). However, these local approaches lack the high-resolution, generalizable, deep learning framework necessary for proactive, centralized forest fire detection, signifying a clear research need.

III. Materials and Methods

This study proposes a cross-sensor transfer learning framework for forest fire detection using DenseNet-121 applied to Landsat-8 and Sentinel-2 imagery. The methodology involves a two-phase training approach: initial feature learning on a large-scale Landsat-8 dataset followed by fine-tuning on localized Sentinel-2 imagery from Benguet, Philippines.

Model performance was evaluated using standard classification metrics, including accuracy, precision, recall, F1-Score, and confusion matrices. To enhance interpretability, Gradient-weighted Class Activation Mapping (Grad-CAM) [38] generated heatmaps highlighting spatial regions contributing most to fire prediction. These heatmaps were further processed to estimate the fire affected area in hectares, linking classification results to severity assessment. This integrated methodology combines detection, visual explainability, and impact assessment, supporting effective deep learning for wildfire monitoring and decision-making. The complete workflow is illustrated in Fig. 1.

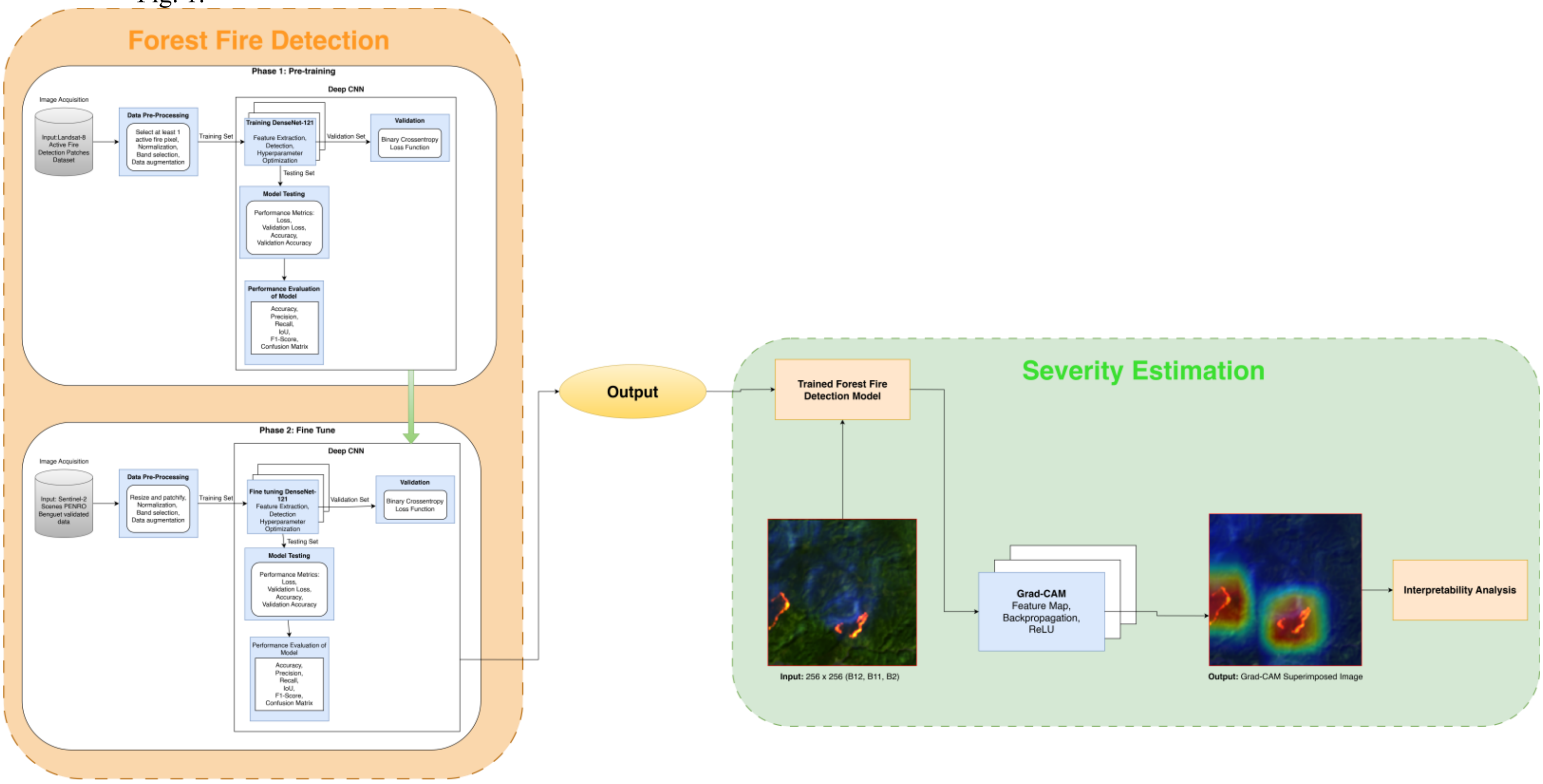

Fig. 1. Overall workflow for forest fire detection and severity estimation.

A. Data Acquisition

This study was conducted in Benguet Province, Cordillera Administrative Region, Philippines with geographic coordinates 16°38'25.9" N, 120°46'30.9" E, a mountainous region spanning elevations of 200-2,900 meters above sea level with 214,523 hectares of forest coverage. The area experiences a Type I climate with dry period from November to April [34].

Two complementary satellite datasets were employed in this study:

- **Landsat-8 Active Fire Patches Dataset:** For model pre-training, the Asia 4 subset dataset developed by Pereira et al. [3] was employed. This dataset was derived from 7,647 initial Landsat-8 Operational Land Imager (OLI) image patches spanning 2013-2018 across fire-prone regions. To ensure labeling accuracy, a voting mechanism was applied where at least two of three established fire detection algorithms [23-25] had to agree on fire presence. This process resulted in 7,647 validated image patches comprising 3,099 fire and 4,548 non-fire instances. Each 256 × 256 pixel patch at 30-meter spatial resolution and includes all OLI spectral bands.

- **Sentinel-2 Local Dataset:** A localized dataset was constructed using Sentinel-2 Level-2A imagery acquired from the Copernicus Open Access Hub. Following consultation with the Department of Environment and Natural Resources - Provincial Environment and Natural Resources Office (DENR-PENRO) in Benguet, 24 scenes with documented fire events occurring between 2019 and 2021 in Benguet, Philippines were identified. From these scenes, 128 image patches with 256×256 pixels at 10-meter resolution were extracted, including 51 fire and 77 non-fire patches.

Both datasets were used to evaluate cross-sensor transfer learning capability, where the model trained on Landsat-8 was adapted for Sentinel-2 imagery.

B. Data Preprocessing

A three-band combination was selected based on established fire detection literature [3]: Short-Wave Infrared 2 (SWIR2) Short-Wave Infrared 1 (SWIR1), and Blue. SWIR bands are essential for detecting thermal anomalies, while the Blue band enhances discrimination of smoke plumes and atmospheric effects associated with active fires. For Landsat-8, bands 7 (SWIR2), 6 (SWIR1), and 2 (Blue) were used. For Sentinel-2, bands 12 (SWIR2), 11 (SWIR1), and 2 (Blue) were employed. This combination effectively captures fire-related spectral signatures while maintaining computational efficiency.

Sentinel-2 image was segmented into 256 × 256 pixel patches aligned with Landsat-8 specifications, followed by normalization using min-max scaling to ensure cross-sensor compatibility. Recognizing the limited availability of annotated satellite datasets for fire detection machine learning applications, systematic data augmentation [39] was applied. Training samples underwent horizontal, vertical, and combined flip transformations, expanding the dataset fourfold and enhancing model capacity to generalize across diverse acquisition conditions and lighting scenarios. To mitigate the risk of overfitting inherent in training deep convolutional networks on limited datasets, a systematic data augmentation strategy was implemented. Given that satellite imagery is rotation-invariant for classification purposes, meaning a fire's spectral signature remains valid regardless of its orientation, geometric transformations were applied to artificially expand the training diversity.

The localized Sentinel-2 dataset consisted of 128 validated image patches (51 fire, 77 non-fire). To ensure rigorous evaluation, these were partitioned into training (70%, n=89), validation (20%, n=26), and testing (10%, n=13) subsets using stratified sampling to maintain class distribution. To address data scarcity, only the training subset (n=89) underwent the augmentation of horizontal, vertical, and combined flips, expanding the training pool by a factor of four to 356 samples (89 x 4). The validation and testing sets remained to ensure the model was evaluated on original, unaltered real-world imagery. Consequently, the final Sentinel-2 dataset structure comprised 395 total patches with 356 training, 26 validation, 13 testing.

The Landsat-8 dataset was partitioned with 70% allocated for combined training and validation and 30% reserved for testing while the Sentinel-2 dataset followed a standard 70%, 20%, 10% split for training, validation, and testing subsets respectively. The combined datasets encompass diverse fire scenarios, including varying fire intensities, atmospheric conditions, acquisition times, and smoke patterns, providing comprehensive representation for model training and assessment.

TABLE I. SUMMARY OF DATA PREPROCESSING WORKFLOW

Step	Parameter / Technique	Details
1. Band Selection	Landsat-8	Bands 7 (SWIR2), 6 (SWIR1), 2 (Blue)
	Sentinel-2	Bands 12 (SWIR2), 11 (SWIR1), 2 (Blue)
2. Spatial Harmonization	Resampling	Sentinel-2 bands (20m) resampled to 10m resolution.
	Patch Extraction	Images segmented into fixed 256 x 256 pixel non-overlapping patches.
3. Normalization	Min-Max Scaling	Pixel values scaled to range to ensure numerical stability and cross-sensor compatibility.
4. Data Augmentation	Techniques	Horizontal Flip, Vertical Flip, Horizontal-Vertical Flip.
	Factor	Original *training* set size increased by 4x (Original + 3 Augmented versions).
	Sentinel-2 Size	128 original patches to 395 augmented *training* set only.
5. Dataset Splitting	Landsat-8	70% Training + Validation / 30% Test.
	Sentinel-2	70% Training / 20% Validation / 10% Test.
6. Labeling Strategy	Binary Classification	Patches labeled as "Fire" or "Non-Fire".
	Ground Truth	Validated via active fire algorithms (Landsat-8) and DENR historical records (Sentinel-2).

C. Model Architecture and Training

DenseNet-121 [18] was selected for its parameter efficiency (7.98M parameters) and superior feature propagation through dense connectivity patterns. The architecture promotes feature reuse and mitigates vanishing gradients, making it well-suited for satellite imagery classification tasks requiring fine-grained feature discrimination. The model was initialized with ImageNet weights and adapted for binary classification (fire vs. non-fire) by adding Global Average Pooling [40], a fully connected layer (256 units, ReLU, L2 regularization) [41], batch normalization, dropout (rate = 0.5) [42], and a sigmoid output layer [43]. The base model layers were frozen during initial training to retain pre-trained features.

Training involved two phases:

1. **Pre-Training:** On Landsat-8 patches using Adam (LR = 0.0001, batch size = 32).

2. **Transfer Learning:** Progressive fine-tuning on Sentinel-2 patches for local adaptation.

Binary cross-entropy was used as the loss function. To further optimize training and improve generalization, callback functions such as early stopping [44], and learning-rate reduction [45]. Also, class weights [45, 46] were applied to address class imbalance. Model performance was evaluated using Accuracy, Precision, Recall, F1-Score, and Confusion Matrix [48].

TABLE II. SUMMARY OF HYPERPARAMETERS

Parameter	Value / Setting	Description
Model Architecture	DenseNet-121	Pre-trained on ImageNet
Input Shape	(256, 256, 3)	3-band composite (SWIR2, SWIR1, Blue)
Batch Size	32	Number of samples processed before model update
Optimizer	Adam	Adaptive Moment Estimation
Learning Rate	0.0001 (1e-4)	Initial learning rate
Loss Function	Binary Cross-Entropy	Standard loss for binary classification
Dropout Rate	0.5	Applied before the output layer to prevent overfitting
L2 Regularization	Enabled	Applied to the fully connected (Dense) layer
Dense Layer Units	256	Number of neurons in the fully connected layer
Activation Function	ReLU	Used in the Dense layer
Output Activation	Sigmoid	Used in the final output layer for binary probability
Class Weights	Applied	To handle class imbalance (Fire vs. Non-Fire)
Early Stopping	Patience = 10	Training stops if validation loss doesn't improve for 10 epochs
LR Reduction	ReduceLROnPlateau	Reduces learning rate when validation metric plateaus

The selection of a transfer learning pathway from Landsat-8 to Sentinel-2 is driven by the availability of high-quality training data and the operational requirements of local fire monitoring. While deep learning models require massive datasets to generalize effectively, such large-scale active fire datasets are scarce for Sentinel-2. Conversely, the Landsat-8 Active Fire Dataset introduced by Pereira et al. [3] provides a globally diverse, large-scale archive of over 150,000 validated patches, serving as an ideal foundation for learning robust, sensor-agnostic spectral features of thermal anomalies. However, for operational deployment in the Philippines, Landsat-8's 16-day revisit cycle is insufficient for capturing forest fire events in cloud-prone tropical regions. Sentinel-2 was therefore selected as the target domain due to its superior 5-day revisit time, which significantly increases the probability of acquiring cloud-free imagery of active fires. By pre-training on the extensive Landsat-8 archive and fine-tuning on the limited local Sentinel-2 samples, the model leverages the best of both worlds.

D. Explainability and Severity Estimation

To provide interpretable insights into model decision-making, Grad-CAM [38] was implemented to visualize spatial regions most influential for fire detection. For each 256 × 256 × 3 input patch, Grad-CAM computes gradients of the fire class score with respect to feature maps from the conv5_block16_concat layer. The method weights each channel by spatially averaged gradients, generating a heatmap resized to match the input dimensions [48-50].

The number of activated blocks is computed as:

$$Number\ of\ blocks = \sum H_{ij} > T \tag{1}$$

where H_{ij} is the value of the heatmap at pixel (i, j) and T is the user-defined threshold with default setting of 0.5.

A unified threshold value of 0.5 was implemented across both model prediction and Grad-CAM analysis to ensure decision consistency. When the DenseNet-121 fire class confidence falls below this threshold, the system reports "No fire detected" without generating area approximations, preventing false alarms from ambiguous features or noise artifacts.

This scaling factor of 32^2 arises from the DenseNet-121 ‘conv5_block16_concat’ layer, where the final convolutional feature map (conv5_block16_concat) has dimensions of 8 × 8 for a 256 × 256 input patch, establishing a direct spatial correspondence of 256 ÷ 8 = 32 pixels per activation block.

The conversion from pixel count to real-world area is based on Sentinel-2's established ground sampling distance specifications [52]. Sentinel-2 imagery provides different spatial resolutions across its spectral bands, with the selected bands having the following characteristics:

- **Blue band (B2):** 10-meter ground resolution
- **SWIR1 band (B11):** 20-meter native resolution, resampled to 10-meter.
- **SWIR2 band (B12):** 20-meter native resolution, resampled to 10-meter.

Since all bands were harmonized to 10-meter resolution during preprocessing, each pixel in the processed imagery represents a ground area of 10 × 10 = 100 square meters. This standardization ensures consistent spatial interpretation across all spectral bands used in the analysis.

The denominator of 10,000 m² converts square meters to hectares, following the standard SI unit conversion where 1 hectare equals 10,000 square meters.

Conversion to pixel count and area follows:

$$N_{FirePixels} = Number\ of\ blocks \times 32^2 \tag{2}$$

$$Area\ per\ pixel = 10 \times 10 = 100\ m^2 \tag{3}$$

$$Fire\ Area\ (ha) = \frac{N_{FirePixels} \times 100\ m^2}{10{,}000\ m^2} \tag{4}$$

Given the ongoing development of the Department of Environment and Natural Resources (DENR) local Forest Fire Danger Rating System (FDRS), severity levels were adapted from established wildfire management literature:

- **Low:** < 10 hectares
- **Moderate:** 10–100 hectares
- **High:** 100–1000 hectares
- **Extreme:** > 1,000–10,000 hectares

This stratification aligns with remote sensing severity estimation approaches and provides operational context for fire management decisions [53].

By combining DenseNet-121's powerful feature extraction, Grad-CAM's interpretability, and area-based severity classification, it established a transparent framework for not only detecting but also quantifying and grading forest fires from satellite imagery.

IV. RESULT AND DISCUSSION

A. Dataset

This study utilized two primary datasets:
(1) a publicly available Landsat-8 Active Fire Detection dataset [3] containing 18, 848 labeled patches after augmentation resulting in 14, 976 training instances with a 39.6% fire to 60.4% non-fire distribution, and (2) a locally collected Sentinel-2 dataset from Benguet, Philippines, comprising 395 augmented patches, wherein only the training instances where augmented from 89 to 356 instances.

The substantial size difference between datasets reflects the scarcity of labeled satellite fire detection datasets in the Philippines emphasizing the value of transfer learning approaches for data-limited scenarios.

B. Model Architecture and Training Configuration

The DenseNet-121 model was configured for binary fire classification, initialized with ImageNet pretrained weights, and input to dimensions (256, 256, 3). Training involved 7,301,185 total parameters, with 263,169 trainable, optimized via Adam (learning rate = 0.0001), employing early stopping, learning rate reduction, and class weights to handle class imbalance.

C. Landsat-8 Baseline Performance Analysis

Fine-tuning DenseNet-121 on the large-scale Landsat-8 dataset established the baseline performance for cross-sensor transfer learning. Training converged at epoch 57 with early stopping (patient=10), indicating effective learning as demonstrated in Fig. 2. The validation loss plateaued at 0.8824, with training loss reaching 0.7889, suggesting appropriate model capacity for the dataset complexity. Learning rate reduction occurred multiple times during training, suggesting adaptive optimization for model refinement.

The model exhibits a generalization gap, with training accuracy reaching approximately 87% while validation accuracy plateaus near 67%. While this indicates some degree of overfitting typical of deep models on noisy remote sensing data, the steady decrease in training loss confirms that the network is successfully learning discriminative spectral features. These learned features such as the relationships between SWIR and Blue bands serve as an initialization for the subsequent transfer learning stage, providing the necessary domain knowledge

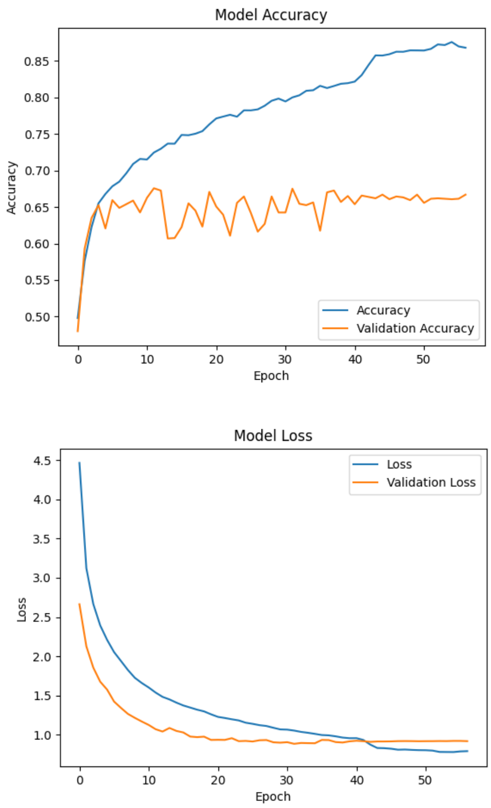

Fig. 2. Model's training performance on base Landsat-8 dataset.

Table III presents comprehensive performance metrics for the Landsat-8 baseline evaluation in the test set (30% of total data, n=2,272).

TABLE III. LANDSAT-8 BASELINE PERFORMANCE METRICS

Metric	Value	Interpretation
Accuracy	66.99%	Moderate overall performance
Precision	62.18%	Acceptable false positive control
Recall	56.24%	Limited fire detection sensitivity
F1-Score	59.06%	Balanced precision-recall trade-off

The model was evaluated using four essential classification metrics: accuracy, precision, recall, and F1-Score. A detailed explanation of each metric is provided below.

- Accuracy indicates the proportion of correct predictions made by the classifier, calculated as the ratio of correctly predicted instances to the total number of predictions.
- Precision represents the fraction of true positive predictions among all positive predictions made by the model.
- Recall measures the fraction of true positive predictions relative to all actual positive cases.

$$Accuracy = \frac{TP+TN}{TP+TN+FP+FN} \quad (5)$$

$$Precision = \frac{TP}{TP+FP} \quad (6)$$

$$Recall = \frac{TP}{TP+FN} \quad (7)$$

Here, TP, TN, FP, and FN correspond to True Positive, True Negative, False Positive, and False Negative, respectively.

- F1-Score is the harmonic mean of precision and recall, providing a balance between the two metrics.

$$F1 = 2 \times \frac{Precision \times Recall}{Precision + Recall} \quad (8)$$

Fig. 3 provides detailed insights into the model's classification performance on the Landsat-8 test dataset. The model achieved 541 TP and 981 TN, demonstrating reasonable capability in correctly identifying both fire and non-fire instances. However, the analysis reveals significant areas for improvement, with 421 FN and 329 FP.

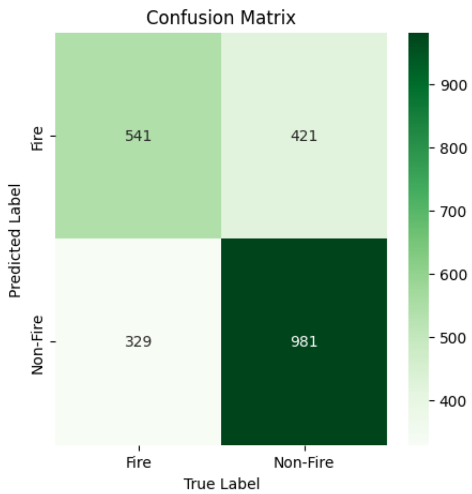

Fig. 3. Model's training performance on base Landsat-8 dataset confusion matrix.

The false negative rate of 43.76% (421/962 actual fire instances) represents a critical limitation, indicating that the model fails to detect approximately 44% of actual fire occurrences. This high miss rate is particularly concerning for operational fire detection systems, where undetected fires can lead to catastrophic consequences.

Conversely, the false positive rate of 25.12% (329/1,310 actual non-fire instances) indicates that the model incorrectly identifies non-fire regions as fire.

TABLE IV. DETAILED CONFUSION MATRIX ANALYSIS

Metric	Count	Percentage of Total
True Positives (TP)	541	23.81%
True Negatives (TN)	981	43.17%
False Positives (FP)	329	14.48%
False Negatives (FN)	421	18.53%

The relatively balanced distribution of errors (FP: 14.48%, FN: 18.53%) suggests that the model does not exhibit strong bias toward either class, though the consequences of false negatives are significantly more severe in fire detection applications. The moderate true positive rate of 56.24% establishes a clear baseline for measuring improvement through cross-sensor transfer learning approaches.

These baseline results underscore the challenge of satellite-based fire detection using traditional training approaches and provide strong justification for implementing cross-sensor transfer learning strategies to enhance model performance, particularly in reducing the critical false negative rate that compromises operational fire detection reliability.

D. Sentinel-2 Direct Transfer Performance

To establish a baseline for transfer learning efficiency, a control experiment was conducted using a direct transfer learning approach. In this setup, the DenseNet-121 model was initialized with ImageNet weights and fine-tuned directly on the Sentinel-2 training dataset, bypassing the intermediate Landsat-8 training phase. This evaluates the model's ability to learn fire features solely from the limited local dataset.

When evaluated on the independent, unseen Sentinel-2 test set (n=72), the direct transfer model achieved an accuracy of 91.67%. While the model demonstrated high precision (100% on internal validation), its performance on the independent set revealed limitations in generalization, yielding an F1-score of 84.21% with 3 false positives and 3 false negatives. These results (detailed in Table IV in Section G) serve as the control baseline to quantify the specific benefits of the proposed cross-sensor domain adaptation strategy.

Fig. 4 illustrates the training and validation curves for the direct transfer control experiment. The Training Accuracy rapidly converges to nearly 100%, while the Validation Accuracy) plateaus at 85% and exhibits significant fluctuations.

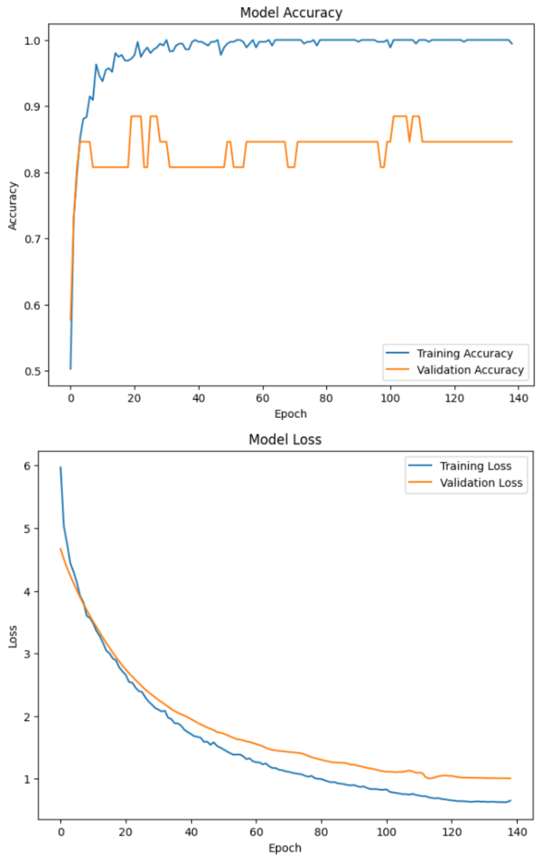

Fig. 4. Local Sentinel-2 dataset model's performance.

E. Cross-Sensor Transfer Learning to Sentinel-2

The pre-trained Landsat-8 model was adapted to Sentinel-2 through progressive fine-tuning. Initially, the last 10 layers were made trainable (converged at epoch 71, validation loss: 0.3002), followed by the last 20 layers (converged at epoch 32, validation loss: 0.2759).

This progressive approach prevented catastrophic forgetting while enabling domain-specific feature adaptation from Landsat-8 to Sentinel-2 spectral characteristics.

Cross-sensor transfer learning achieved remarkable performance gains on Sentinel-2: 97.06% accuracy, 80% precision, 100% recall, and 88% F1-score. This represents

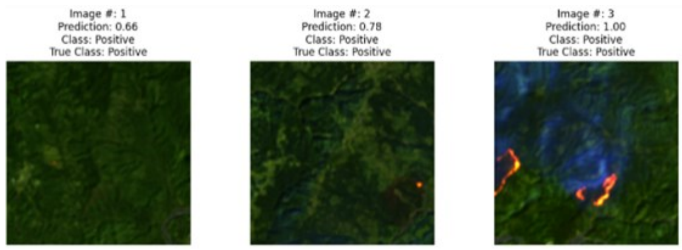

substantial improvement over the Landsat-8 baseline of 66.99% accuracy.

Visualization of learned features Fig. 5. confirms the model correctly identifies fire pixels in high-confidence predictions. Error analysis on Fig. 6. reveals the model occasionally misclassifies water bodies as fire regions, indicating spectral similarity challenges.

Fig. 5. Output of images above 50% classification threshold

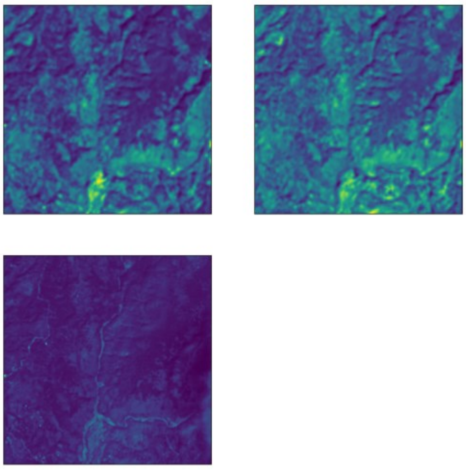

Fig. 6. Visualization of feature maps in 'input_3' layer of the false positive image (60%) of the test set.

F. Independent validation

To assess real-world applicability, an unseen Sentinel-2 (2023-03-23-00_00_2023-03-23-23_59_Sentinel-2_L2A) [54] scene was evaluated independently. The fine-tuned model maintained strong performance with 94.44% accuracy, 89.47% precision, 89.47% recall, and 89.47% F1-score.

Fig. 7. Independent validation confusion matrix showing maintained performance on unseen Sentinel-2 data.

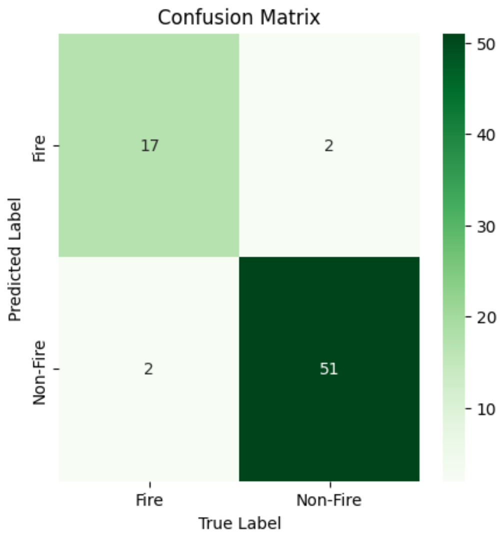

Fig. 7. Independent validation confusion matrix.

While the model achieved high accuracy on the independent validation set, it is important to acknowledge the limitations regarding the spatiotemporal diversity of this test data. The independent evaluation relied on a Sentinel-2 scene from a single date (March 24, 2023). Although this confirms the model's ability to generalize unseen data within that specific temporal window and geographic context, it may not fully capture the variability of fire signatures under different seasonal lighting conditions or vegetation moisture levels. Future work will focus on seasonal susceptibility fire maps that could be generated by training the model on these seasonal datasets to predict areas that are more likely to catch fire during certain periods of the year.

G. Comparative Analysis and Transfer Learning Impact

The proposed DenseNet-121 framework demonstrated significant performance enhancement through the two-stage cross-sensor transfer learning strategy. To quantify this improvement, the proposed method was compared against the control baseline on the same independent test set.

Table V summarizes the comparative performance. The proposed method outperformed the direct transfer control across all key metrics.

As shown in Table V, the direct transfer model achieved an F1-score of 84.21% with a balanced but higher error rate (3 false positives, 3 false negatives). In contrast, the proposed method improved the F1-score to 89.47%, reducing both false positives and false negatives to 2. This +5.26% improvement in F1-score confirms that the intermediate training on the large-scale Landsat-8 dataset effectively transferred sensor-agnostic spectral features, enabling the model to generalize better to unseen Sentinel-2 imagery than could be achieved by using the limited local dataset alone.

TABLE V. PERFORMANCE COMPARISON OF DIRECT TRANSFER VS. PROPOSED METHOD ON UNSEEN DATA

Metric	Direct Transfer (Sentinel-2)	After Fine-Tuning (Sentinel-2)	Improvement
Accuracy	91.67%	94.44%	+2.77%
Precision	84.21%	89.47%	+5.26%
Recall	84.21%	89.47%	+5.26%
F1-Score	84.21%	89.47%	+5.26%

The DenseNet-121 model demonstrated significant performance enhancement through cross-sensor transfer learning. Baseline Landsat-8's performance (83.34% accuracy) improved substantially when transferred to Sentinel-2, achieving 94.44% accuracy on unseen data.

Furthermore, Table VI highlights the impact of fine-tuning relative to the initial Landsat-8 baseline and summarizes the quantitative improvements after fine-tuning. Most notably, precision increased from 61.29% to 89.47% (+28.18%), indicating superior false positive reduction, critical for operational fire detection systems.

The slight recall decline (10.53%) reflects conservative model behavior, trading minimal fire detection sensitivity for dramatic false positive reduction, enhancing overall system reliability. This trade-off benefits operational deployment where false alarms incur significant resource allocation costs. The F1-score improvement (+13.47%) confirms overall classification enhancement.

The substantial metric improvements validate the effectiveness of cross-sensor domain adaptation. The model successfully leveraged Landsat-8 learned features for Sentinel-2 imagery, demonstrating DenseNet-121's capability for multi-sensor fire detection applications.

TABLE VI. PERFORMANCE COMPARISON OF BEFORE AND AFTER FINE TUNING OF THE MODEL ON UNSEEN DATA

Metric	Before Fine-Tuning (Landsat-8)	After Fine-Tuning (Sentinel-2)	Difference	Impact of Fine-Tuning
Accuracy	83.34%	94.44%	+11.10%	Improved
Precision	61.29%	89.47%	+28.18%	Improved
Recall	100%	89.47%	-10.53%	Declined
F1-Score	76%	89.47%	+13.47%	Improved

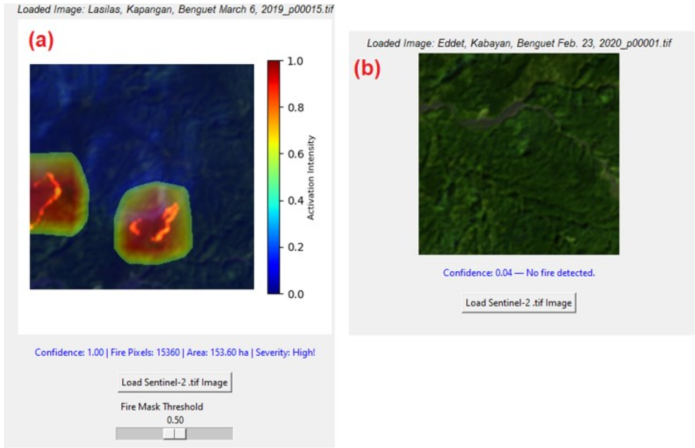

Fig. 9. (a) Example of satellite image that detected fire with the Grad-CAM fire masks. (b) Example of satellite image with no fire

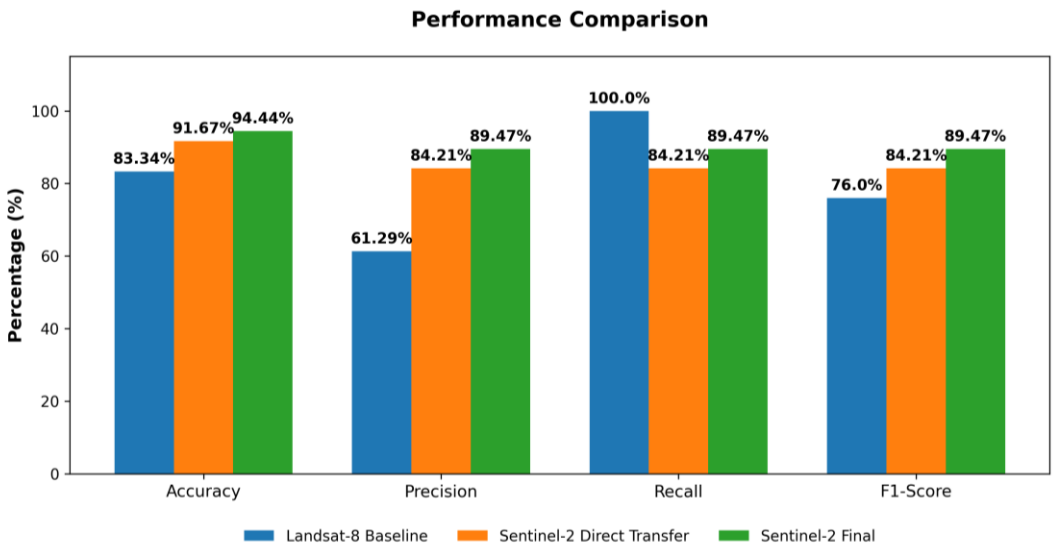

Fig. 8. Performance Comparison DenseNet-121 Fine-Tuning Impact on Unseen Sentinel-2 Data

H. Grad-CAM-Based Fire Severity Classification and Spatial Analysis

The integration of Grad-CAM with DenseNet-121 provided interpretable visual explanations for fire detection decisions. Grad-CAM generates heatmaps highlighting regions that most significantly contribute to classification, with red-intensity values indicating model confidence for fire presence as shown in Fig. 9. [38].

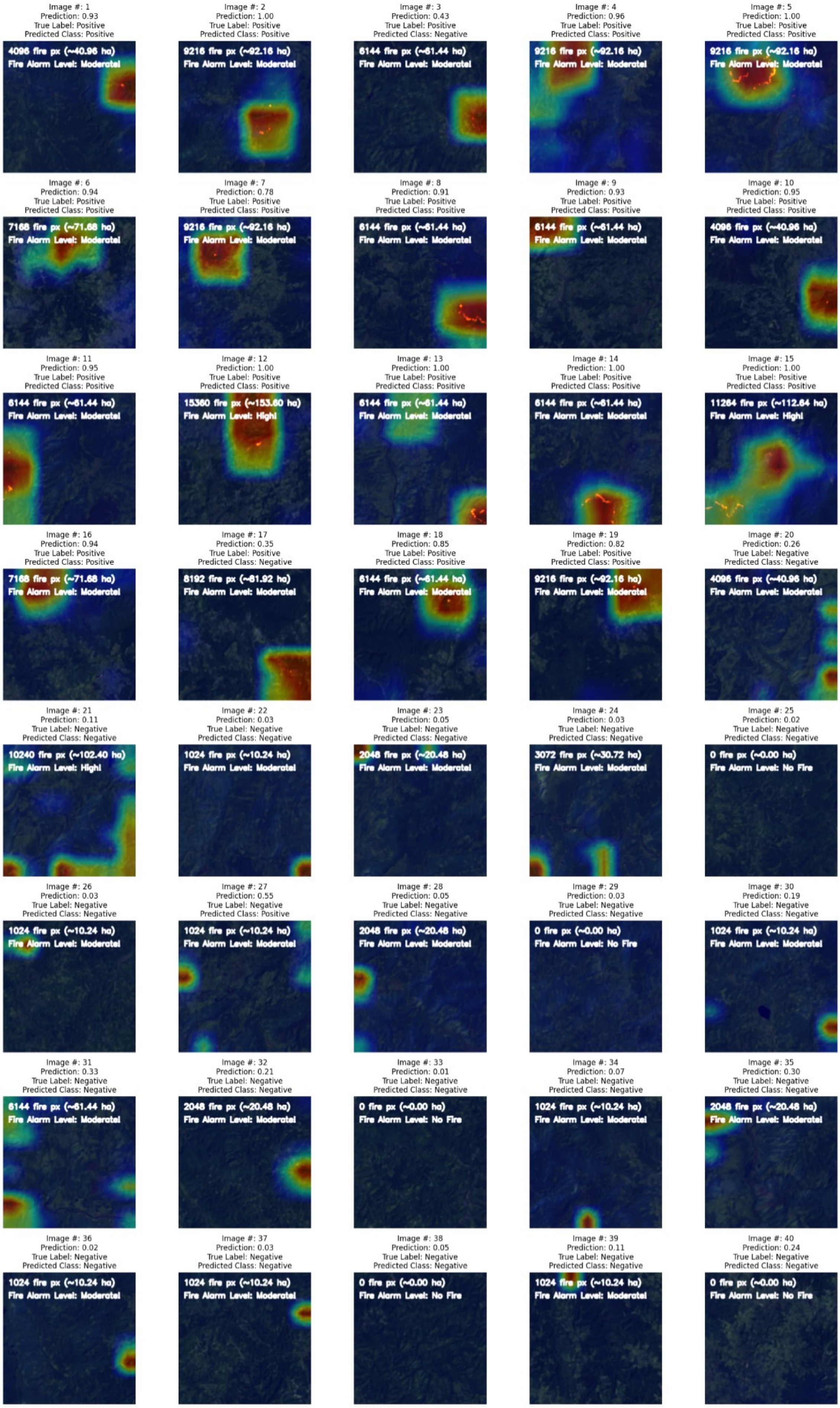

Fig. 10. 40 patches output of the model + superimposed Grad-CAM on Sentinel-2 unseen set

Fire-affected pixels were identified using threshold T = 0.50, corresponding to the DenseNet-121 decision boundary.

Fig. 10. Demonstrates consistent Grad-CAM activation patterns across all 72 Sentinel-2 patches, validating the model's spatial attention mechanism and providing quantitative fire impact assessments for operational deployment.

The successful deployment of this cross-sensor model offers immediate operational benefits for agencies like DENR. By utilizing freely available Sentinel-2 imagery (5-day revisit), this system can function as a cost-neutral virtual forest watcher, prioritizing high-risk alerts for human verification. The interpretability provided by the Grad-CAM heatmaps allows non-technical personnel to quickly assess fire size and location, streamlining the decision-making process for dispatching firefighting resources to rugged, inaccessible terrain in the Cordillera region.

V. Conclusion

This study successfully demonstrates DenseNet-121's effectiveness for cross-sensor forest fire detection using Landsat-8 and Sentinel-2 satellite imagery in Benguet, Philippines. The research achieved both primary objectives: local fine-tuning improved model performance to 89.47% F1-score on unseen data, while cross-sensor transfer learning proved highly effective across different satellite platforms.

The integration of cross-sensor transfer learning with Gradient-weighted Class Activation Mapping creates a novel framework bridging binary classification and operational fire assessment. This approach transforms neural network outputs into interpretable spatial visualizations and quantitative severity estimates from low to catastrophic levels.

The developed system provides high detection accuracy with spatial interpretability, addressing critical gaps in real-time fire monitoring. The severity classification framework enables prioritized emergency response and resource allocation decisions.

This work establishes a scalable methodology for remote sensing environmental monitoring in data-scarce regions. The cross-sensor approach opens possibilities for leveraging multi-platform satellite data, extending to other environmental applications. The combination of high performance with explainable AI creates a foundation for next-generation disaster response systems.

Conflict of Interest

The authors declare no conflict of interest.

Author Contributions

Lance Asher M. Elloso was responsible for *conceptualization*, *feasibility analysis*, and the *application of the DenseNet-121 convolutional neural network (CNN)*. Also, carried out the *methodology design*, *data curation*, *experimentation*, and *interpretation of results*. Khristine F. Mecija contributed to *writing – review and editing*, including *proofreading*, *cross-referencing, and final revision* of the manuscript, with the assistance of Estefanee Ashley N. Garcia. John Paul Q. Tomas *supervised the research and revised the manuscript*. All authors read and had approved the final version.

Acknowledgment

The authors would like to express their gratitude to the [redacted] for providing the local dataset essential to this study. We also acknowledge the [redacted] for their valuable consultation, and the [redacted] for the provision of secondary data.

References

[1] C. Aponte, W. J. De Groot, and B. M. Wotton, "Forest fires and climate change: causes, consequences and management options," *Int. J. Wildland Fire*, vol. 25, no. 8, p. i, 2016, doi: 10.1071/WFv25n8_FO.

[2] R. J. Keenan, "Climate change impacts and adaptation in forest management: a review," *Annals of Forest Science*, vol. 72, no. 2, pp. 145–167, Mar. 2015, doi: 10.1007/s13595-014-0446-5.

[3] G. H. De Almeida Pereira, A. M. Fusioka, B. T. Nassu, and R. Minetto, "Active fire detection in Landsat-8 imagery: A large-scale dataset and a deep-learning study," *ISPRS Journal of Photogrammetry and Remote Sensing*, vol. 178, pp. 171–186, Aug. 2021, doi: 10.1016/j.isprsjprs.2021.06.002.

[4] R. Ghali and M. A. Akhloufi, "Deep Learning Approaches for Wildland Fires Using Satellite Remote Sensing Data: Detection, Mapping, and Prediction," *Fire*, vol. 6, no. 5, p. 192, May 2023, doi: 10.3390/fire6050192.

[5] S. T. Seydi, V. Saeidi, B. Kalantar, N. Ueda, and A. A. Halin, "Fire-Net: A Deep Learning Framework for Active Forest Fire Detection," *Journal of Sensors*, vol. 2022, pp. 1–14, Feb. 2022, doi: 10.1155/2022/8044390.

[6] L. Zhao, J. Liu, S. Peters, J. Li, S. Oliver, and N. Mueller, "Investigating the Impact of Using IR Bands on Early Fire Smoke Detection from Landsat Imagery with a Lightweight CNN Model," *Remote Sensing*, vol. 14, no. 13, p. 3047, Jun. 2022, doi: 10.3390/rs14133047.

[7] Y. Wang, X. Liu, M. Li, W. Di, and L. Wang, "Deep Convolution and Correlated Manifold Embedded Distribution Alignment for Forest Fire Smoke Prediction," *cai*, vol. 39, no. 1–2, pp. 318–339, 2020, doi: 10.31577/cai_2020_1-2_318.

[8] R. Ba, C. Chen, J. Yuan, W. Song, and S. Lo, "SmokeNet: Satellite Smoke Scene Detection Using Convolutional Neural Network with Spatial and

Channel-Wise Attention," *Remote Sensing*, vol. 11, no. 14, p. 1702, Jul. 2019, doi: 10.3390/rs11141702.

[9] T. C. Phan and T. T. Nguyen, "Remote Sensing meets Deep Learning: Exploiting Spatio-Temporal-Spectral Satellite Images for Early Wildfire Detection", [Online]. Available: https://api.semanticscholar.org/CorpusID:204746641

[10] Z. Hong *et al.*, "Active Fire Detection Using a Novel Convolutional Neural Network Based on Himawari-8 Satellite Images," *Front. Environ. Sci.*, vol. 10, p. 794028, Mar. 2022, doi: 10.3389/fenvs.2022.794028.

[11] D. Rashkovetsky, F. Mauracher, M. Langer, and M. Schmitt, "Wildfire Detection From Multisensor Satellite Imagery Using Deep Semantic Segmentation," *IEEE J. Sel. Top. Appl. Earth Observations Remote Sensing*, vol. 14, pp. 7001–7016, 2021, doi: 10.1109/JSTARS.2021.3093625.

[12] F. Li, R. Feng, W. Han, and L. Wang, "High-Resolution Remote Sensing Image Scene Classification via Key Filter Bank Based on Convolutional Neural Network," *IEEE Trans. Geosci. Remote Sensing*, vol. 58, no. 11, pp. 8077–8092, Nov. 2020, doi: 10.1109/TGRS.2020.2987060.

[13] C. Sun, "Analyzing Multispectral Satellite Imagery of South American Wildfires Using Deep Learning," in *2022 International Conference on Applied Artificial Intelligence (ICAPAI)*, Halden, Norway: IEEE, May 2022, pp. 1–6. doi: 10.1109/ICAPAI55158.2022.9801567.

[14] L. Knopp, M. Wieland, M. Rättich, and S. Martinis, "A Deep Learning Approach for Burned Area Segmentation with Sentinel-2 Data," *Remote Sensing*, vol. 12, no. 15, p. 2422, Jul. 2020, doi: 10.3390/rs12152422.

[15] Z. Wang *et al.*, "Semantic Segmentation and Analysis on Sensitive Parameters of Forest Fire Smoke Using Smoke-Unet and Landsat-8 Imagery," *Remote Sensing*, vol. 14, no. 1, p. 45, Dec. 2021, doi: 10.3390/rs14010045.

[16] A. Rostami, R. Shah-Hosseini, S. Asgari, M. Aghdami-Nia, and S. Homayouni, "Active Fire Detection from Landsat-8 Imagery Using Deep Multiple Kernel Learning," 2022, doi: https://doi.org/10.3390/rs14040992.

[17] "Forest Fire Management Information System (FFMIS)." Asian Forest Cooperation Organization (AFoCO), 2022. [Online]. Available: https://afocosec.org/wp-content/uploads/2022/05/KN2022-006-Forest-Fire-Management-Information-System-FFMIS-20220531-2.pdf

[18] G. Huang, Z. Liu, G. Pleiss, L. V. D. Maaten, and K. Q. Weinberger, "Convolutional Networks with Dense Connectivity," *IEEE Trans. Pattern Anal. Mach. Intell.*, vol. 44, no. 12, pp. 8704–8716, Dec. 2022, doi: 10.1109/TPAMI.2019.2918284.

[19] A. A. Adegun, S. Viriri, and J.-R. Tapamo, "Review of deep learning methods for remote sensing satellite images classification: experimental survey and comparative analysis," *J Big Data*, vol. 10, no. 1, p. 93, Jun. 2023, doi: 10.1186/s40537-023-00772-x.

[20] M. M. Stofa, M. A. Zulkifley, and S. Z. Muhammad Zaki, "A deep learning approach to ship detection using satellite imagery," *IOP Conf. Ser.: Earth Environ. Sci.*, vol. 540, no. 1, p. 012049, Jul. 2020, doi: 10.1088/1755-1315/540/1/012049.

[21] R. Minetto, M. Pamplona Segundo, and S. Sarkar, "Hydra: An Ensemble of Convolutional Neural Networks for Geospatial Land Classification," *IEEE Trans. Geosci. Remote Sensing*, vol. 57, no. 9, pp. 6530–6541, Sep. 2019, doi: 10.1109/TGRS.2019.2906883.

[22] A. A. A. Alkhatib, "A Review on Forest Fire Detection Techniques," *International Journal of Distributed Sensor Networks*, vol. 10, no. 3, p. 597368, Mar. 2014, doi: 10.1155/2014/597368.

[23] W. Schroeder, P. Oliva, L. Giglio, B. Quayle, E. Lorenz, and F. Morelli, "Active fire detection using Landsat-8/OLI data," *Remote Sensing of Environment*, vol. 185, pp. 210–220, Nov. 2016, doi: 10.1016/j.rse.2015.08.032.

[24] S. W. Murphy, C. R. De Souza Filho, R. Wright, G. Sabatino, and R. Correa Pabon, "HOTMAP: Global hot target detection at moderate spatial resolution," *Remote Sensing of Environment*, vol. 177, pp. 78–88, May 2016, doi: 10.1016/j.rse.2016.02.027.

[25] S. S. Kumar and D. P. Roy, "Global operational land imager Landsat-8 reflectance-based active fire detection algorithm," *International Journal of Digital Earth*, vol. 11, no. 2, pp. 154–178, Feb. 2018, doi: 10.1080/17538947.2017.1391341.

[26] M. Nabi and I. Bordanov, "Research of Forest Fire Detection on Satellite Images," in *2023 International Conference on Industrial Engineering, Applications and Manufacturing (ICIEAM)*, Sochi, Russian Federation: IEEE, May 2023, pp. 803–808. doi: 10.1109/ICIEAM57311.2023.10139138.

[27] J. Deng, W. Dong, R. Socher, L.-J. Li, Kai Li, and Li Fei-Fei, "ImageNet: A large-scale hierarchical image database," in *2009 IEEE Conference on Computer Vision and Pattern Recognition*, Miami, FL: IEEE, Jun. 2009, pp. 248–255. doi: 10.1109/CVPR.2009.5206848.

[28] R. S. Priya and K. Vani, "Deep Learning Based Forest Fire Classification and Detection in Satellite Images," in *2019 11th International Conference on Advanced Computing (ICoAC)*, Chennai, India: IEEE, Dec. 2019, pp. 61–65. doi: 10.1109/ICoAC48765.2019.246817.

[29] G. Christie, N. Fendley, J. Wilson, and R. Mukherjee, "Functional Map of the World," in *2018 IEEE/CVF Conference on Computer Vision and Pattern Recognition*, Salt Lake City, UT, USA:

IEEE, Jun. 2018, pp. 6172–6180. doi: 10.1109/CVPR.2018.00646.
[30] M. Iman, H. R. Arabnia, and K. Rasheed, "A Review of Deep Transfer Learning and Recent Advancements," *Technologies*, vol. 11, no. 2, p. 40, Mar. 2023, doi: 10.3390/technologies11020040.
[31] R. Raman, W. Jiang, and S. Bakshi, "PODE: Panoptic-Aware Object-Wise Depth Estimation for Occlusion Prediction," *IEEE Trans. Consumer Electron.*, pp. 1–1, 2025, doi: 10.1109/TCE.2025.3610083.
[32] D. López-Puigdollers, G. Mateo-García, and L. Gómez-Chova, "Benchmarking Deep Learning Models for Cloud Detection in Landsat-8 and Sentinel-2 Images," *Remote Sensing*, vol. 13, no. 5, p. 992, Mar. 2021, doi: 10.3390/rs13050992.
[33] L. Zhao, J. Liu, S. Peters, J. Li, N. Mueller, and S. Oliver, "Cross-sensor transfer learning for fire smoke scene detection using variable-bands multi-spectral satellite imagery aided by spectral patterns," *International Journal of Remote Sensing*, vol. 45, no. 10, pp. 3332–3348, May 2024, doi: 10.1080/01431161.2024.2343430.
[34] C. Poclis, C. Tiburan Jr, D. Racelis, R. Visco, M. Galang, and J. Villareal, "Comparative Analysis of Different Forest Fire Susceptibility Models in Benguet, the Philippines," *Philipp J Sci*, vol. 153, no. 4, Aug. 2024, doi: 10.56899/153.04.05.
[35] A. J. Sabuito, C. P. Canlas, M. J. Felix, and G. J. Perez, "BENGUET FOREST FIRE BURNED AREA & TAAL ASH EXTENT ESTIMATION USING SUPPORT VECTOR MACHINE & THRESHOLDING TECHNIQUES," 2020.
[36] A. B. Baloloy, A. C. Blanco, B. S. Gana, R. C. Sta. Ana, and L. C. Olalia, "LANDSAT-BASED DETECTION AND SEVERITY ANALYSIS OF BURNED SUGARCANE PLOTS IN TARLAC, PHILIPPINES USING DIFFERENCED NORMALIZED BURN RATIO (dNBR)," *Int. Arch. Photogramm. Remote Sens. Spatial Inf. Sci.*, vol. XLII-4/W1, pp. 173–179, Sep. 2016, doi: 10.5194/isprs-archives-XLII-4-W1-173-2016.
[37] J. R. Asor, J. L. Lerios, S. B. Sapin, J. O. Padallan, and C. A. C. Buama, "Fire incidents visualization and pattern recognition using machine learning algorithms," *IJEECS*, vol. 22, no. 3, p. 1427, Jun. 2021, doi: 10.11591/ijeecs.v22.i3.pp1427-1435.
[38] R. R. Selvaraju, M. Cogswell, A. Das, R. Vedantam, D. Parikh, and D. Batra, "Grad-CAM: Visual Explanations from Deep Networks via Gradient-based Localization," 2016, doi: 10.48550/ARXIV.1610.02391.
[39] C. Shorten and T. M. Khoshgoftaar, "A survey on Image Data Augmentation for Deep Learning," *J Big Data*, vol. 6, no. 1, p. 60, Dec. 2019, doi: 10.1186/s40537-019-0197-0.
[40] "Introduction to Pooling Layer," GeeksforGeeks. [Online]. Available: https://www.geeksforgeeks.org/cnn-introduction-to-pooling-layer/
[41] "What is Fully Connected Layer in Deep Learning?," GeeksforGeeks. [Online]. Available: https://www.geeksforgeeks.org/what-is-fully-connected-layer-in-deep-learning/
[42] V. S. Mudigonda, "Understanding Dropout in Deep Neural Networks," 2021, [Online]. Available: https://medium.com/codex/understanding-dropout-in-deep-neural-networks-95e7d1b11c58
[43] J. Brownlee, "How to Choose an Activation Function for Deep Learning," 2021, [Online]. Available: https://medium.com/codex/understanding-dropout-in-deep-neural-networks-95e7d1b11c58
[44] J. Brownlee, "Use Early Stopping to Halt the Training of Neural Networks At the Right Time," 2020, [Online]. Available: https://machinelearningmastery.com/how-to-stop-training-deep-neural-networks-at-the-right-time-using-early-stopping/
[45] R. Heckel and F. F. Yilmaz, "Early Stopping in Deep Networks: Double Descent and How to Eliminate it," Sep. 19, 2020, *arXiv*: arXiv:2007.10099. doi: 10.48550/arXiv.2007.10099.
[46] B. Bakirarar and A. H. Elhan, "Class Weighting Technique to Deal with Imbalanced Class Problem in Machine Learning: Methodological Research," *Turkiye Klinikleri J Biostat*, vol. 15, no. 1, pp. 19–29, 2023, doi: 10.5336/biostatic.2022-93961.
[47] Kamaldeep, "How to Improve Class Imbalance using Class Weights in Machine Learning?," *Analytics Vidhya*, 2025, [Online]. Available: https://www.analyticsvidhya.com/blog/2020/10/improve-class-imbalance-class-weights/
[48] M. Sokolova, N. Japkowicz, and S. Szpakowicz, "Beyond Accuracy, F-Score and ROC: A Family of Discriminant Measures for Performance Evaluation," in *AI 2006: Advances in Artificial Intelligence*, vol. 4304, A. Sattar and B. Kang, Eds., in Lecture Notes in Computer Science, vol. 4304. , Berlin, Heidelberg: Springer Berlin Heidelberg, 2006, pp. 1015–1021. doi: 10.1007/11941439_114.
[49] S. Yin, L. Wang, M. Shafiq, L. Teng, A. A. Laghari, and M. F. Khan, "G2Grad-CAMRL: An Object Detection and Interpretation Model Based on Gradient-Weighted Class Activation Mapping and Reinforcement Learning in Remote Sensing Images," *IEEE J. Sel. Top. Appl. Earth Observations Remote Sensing*, vol. 16, pp. 3583–3598, 2023, doi: 10.1109/JSTARS.2023.3241405.
[50] L. Qiao *et al.*, "Grad-CAM for Network Models: To Support Aerial Vision Based Wildfire Perception," in *IECON 2024 - 50th Annual Conference of the IEEE Industrial Electronics Society*, Chicago, IL, USA: IEEE, Nov. 2024, pp. 1–6. doi: 10.1109/IECON55916.2024.10905147.
[51] T. Sultan, M. S. Chowdhury, M. Safran, M. F. Mridha, and N. Dey, "Deep Learning-Based Multistage Fire Detection System and Emerging

Direction," *Fire*, vol. 7, no. 12, p. 451, Nov. 2024, doi: 10.3390/fire7120451.
[52] European Space Agency, "S2 Mission," *Copernicus*, [Online]. Available: https://sentiwiki.copernicus.eu/web/s2-mission#S2Mission-SpectralResolutionS2-Mission-Spectral-Resolution
[53] S. Monaco *et al.*, "Attention to Fires: Multi-Channel Deep Learning Models for Wildfire Severity Prediction," *Applied Sciences*, vol. 11, no. 22, p. 11060, Nov. 2021, doi: 10.3390/app112211060.
[54] "March 24, 2023 - Fires in the Philippines," *Moderate Resolution Imaging Spectroradiometer Land Rapid Response Team*, vol. National Aeronautics and Space Administration Goddard Space Flight Center (NASA GSFC), [Online]. Available: https://modis.gsfc.nasa.gov/gallery/individual.php?db_date=2023-03-24